Preprogrammed 2D Folding of Conformationally Flexible Oligoamides: Foldamers with Multiple Turn Elements

Cristian Gobbo,[†,§] Min Li,[‡,§,⊥] Kunal S. Mali,[‡,*] Jan H. van Esch,[†,*] and Steven De Feyter[‡,*]

[†]Department of Chemistry, Laboratory of Self-assembling Systems, Delft University of Technology, Julianalaan 136, 2628 BL Delft, The Netherlands and [‡]Division of Molecular Imaging and Photonics, Department of Chemistry, KU Leuven-University of Leuven, Celestijnenlaan 200F, B 3001, Leuven, Belgium. [§]These authors contributed equally. [⊥]Present address: CAS Key Laboratory for Biomedical Effects of Nanomaterials and Nanosafety, Institute of High Energy Physics, Chinese Academy of Sciences, Beijing 100049, China.

ABSTRACT

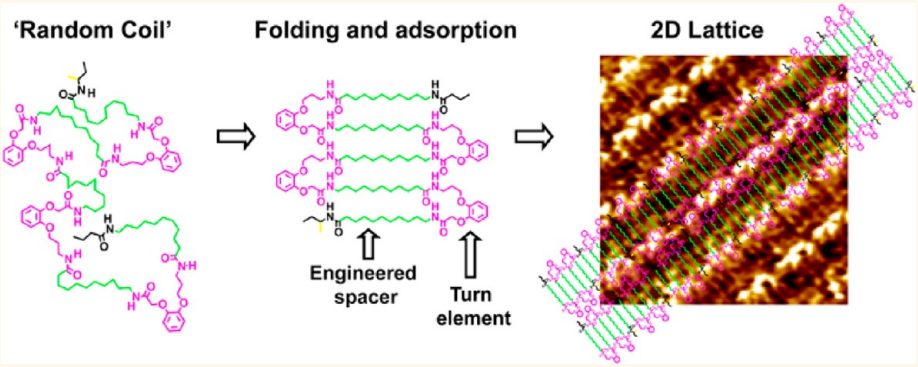

Controlling the molecular conformation of oligomers on surfaces through noncovalent interactions symbolizes an important approach in the bottom-up patterning of surfaces with nanoscale precision. Here we report on the design, synthesis, and scanning tunneling microscopy (STM) investigation of linear oligoamides adsorbed at the liquid–solid interface. A new class of extended foldamers comprising as many as four turn elements based on a structural design "rule" adapted from a mimic foldamer was successfully synthesized. The self-assembly of these progressively complex oligomeric structures was scrutinized at the liquid–solid interface by employing STM. Submolecularly resolved STM images of foldamers reveal characteristic in-plane folding and self-assembly behavior of these conformationally flexible molecules. The complexity of the supramolecular architectures increases with increasing number of turn elements. The dissimilarity in the adsorption behavior of different foldamers is discussed qualitatively in light of enthalpic and entropic factors. The modular construction of these oligomeric foldamers with integrated functionalities provides a simple, efficient, and versatile approach to surface patterning with molecular precision.

KEYWORDS: foldamers · surface patterning · STM · liquid–solid interface

The patterning of surfaces by molecular self-assembly is attracting considerable attention as an alternative to top-down approaches, as it promises unprecedented control over the spatial deposition of chemical functionalities at the nanometer length scale.[1−3] Self-assembled physisorbed monolayers consist of regular 2D lattices of molecules that could be fabricated under ambient conditions at the liquid–solid and air–solid interface or under ultra-high-vacuum (UHV) conditions at the UHV–solid interface. A wide variety of structurally very diverse molecular monolayers have been reported, including simple 2D lamellar structures, single components to sophisticated multicomponent rosettes, nanoporous networks, and hierarchically structured monolayers.[4−12] Despite these advances, approaches that allow the spatial deposition of different chemical functionalities in arbitrary arrangements of 0.2−20 nm sized unit cells remain scarce.[13−15] For example, Buck *et al.*[14] realized a fabrication platform by combining noncovalent self-assembly of porous supramolecular networks and thiol self-assembled monolayers (SAMs) on gold substrates. The porous networks provided nanometer-scale precision, whereas the thiol SAMs allowed for versatile

* Address correspondence to Kunal.Mali@chem.kuleuven.be, J.H.vanEsch@tudelft.nl, Steven.DeFeyter@chem.kuleuven.be.

Received for review August 23, 2012 and accepted November 28, 2012.

Published online November 28, 2012
10.1021/nn303868q

functionalization. Grill *et al.*[15] demonstrated that *trans*-azobenzene derivatives adsorbed in a homogeneous 2D monolayer could be collectively switched with high spatial selectively, thus forming periodically switchable arrays of molecules wherein it is possible to address single functional molecules. Another popular approach is DNA origami,[16−18] where the specificity of the interactions between complementary base pairs of DNA is exploited to enable precise folding of DNA in order to create arbitrary two- and three-dimensional shapes. However, lack of (sub)-nanometric resolution, large surface corrugation of DNA, and limited range of active functionalities limit its application in patterning at the lower end of the nanoscale.

Recently, we introduced surface-confined foldamers as a genuine bottom-up approach for molecular patterning in which linear sequences of building blocks were made to fold and assemble into well-defined 2D patterns upon physisorption at the liquid−solid interface.[19,20] In principle, such surface-confined foldamers allow programming of the folding pattern, shape, and chemical functionalities at the sequence level, whereas its 2D confinement greatly facilitates rational design. The concept of such synthetic foldamers[21−24] is largely inspired from biopolymers such as proteins, which exhibit remarkable capabilities such as molecular recognition, catalysis, and information storage, which in turn are dependent on their compact solution structures with conformational uniqueness.[25−27] We reasoned that this concept, when applied to synthetic foldamers on surfaces, will allow a precise control over positioning of functional groups in a spatially resolved manner, and it is from such well-ordered information-rich surfaces that properties such as affinity, reactivity, and catalytic selectivity will evolve, hence the interest in surface-confined foldamers.[19,20]

In fact, peptides are known to exhibit highly organized assemblies and surface-induced folding.[28−32] Mao *et al.*[33] provided molecular level evidence of the surface-induced transformation of polypeptides by employing scanning tunneling microscopy (STM). Their investigation revealed that although the polypeptide is originally stable with α-helical conformation both in solution and in its crystal state, it forms β-sheet-like assemblies upon adsorption on the graphite surface. The β-sheet structures of amyloid β peptides have also been visualized recently on the surface of highly oriented pyrolytic graphite (HOPG) by using STM under ambient conditions.[34,35] Kern *et al.*[36] obtained submolecularly resolved images of folded and unfolded cytochrome *c* protein ions by using STM under UHV conditions. The self-assembly process of the peptide strands however led to formation of irregular patches.[36] These examples further suggest the possibility of 2D confined folding of peptides into regular 2D structures as an alternative approach for the fabrication of functional molecular surfaces. However, finding appropriate sequences capable of 2D folding will require substantial effort, and one of the straightforward ways is to design and synthesize oligomeric sequences of building blocks that could be preprogrammed to fold upon surface confinement.

Recent attempts toward fully synthetic surface-confined foldamers include the work by Shen *et al.*[37] and Jester *et al.*[38,39] involving the formation of well-ordered physisorbed monolayers formed from both rigid and shape-persistent oligo(phenylene acetylenes), respectively. Shen *et al.*[37] studied the self-assembly and unfolding process of a foldable oligomer made up of alternating units of *ortho*-phenyleneethylene (*o*-PE) and *para*-phenyleneethylene (*p*-PE) at the liquid−graphite interface by employing STM. Since the *o*-PE-*p*-PE segments can exist in *cisoid* or *transoid* states, these oligomers were found to exhibit several different molecular conformations.[37] Jester *et al.*[38,39] synthesized and investigated a series of shape-persistent phenylene−ethynylene−butadiynylene (PEB) oligomers connected by flexible aliphatic linkers. STM revealed that both cyclic and acyclic PEB oligomers could form stable self-assembled monolayers at the liquid−solid interface.[38,39] However, both the systems described above offered only modest control over the remaining degrees of conformational freedom, presumably due to the lack of intramolecular interactions, leading to rich polymorphism and consequently frustrating the expected design of surface patterns.

In our research toward spatially controlled deposition of chemical functionalities within the 0.2−20 nm regime, we have developed surface-confined turn mimics based on catechol bis-amides as a first and essential step toward surface-confined oligo-amide foldamers.[19,20] More recently, we also studied the impact of interaction complementarity and chirality on order and disorder in 2D ribbons of linear bis-amides.[40] Building on these studies, we now report on the design and 2D folding behavior of progressively complex foldamers (Figure 1a), which are evaluated for their in-plane folding behavior upon physisorption at the liquid−solid interface using STM. At this stage, this approach is somewhat limited to HOPG as a substrate, and testing the viability of foldamers for functionalization of other substrates such as metal and semiconductor surfaces calls for elaborate investigations in the future. Nevertheless, it is reasonable to assume that this strategy will be readily applicable for functionalization of similar yet technologically relevant substrates such as graphene. In general, this system represents a promising foundation for developing strategies useful in controlled positioning of functional elements on surfaces and symbolizes an important step toward "directed bottom-up self-assembly" of molecular components.

RESULTS AND DISCUSSION

Design. Our previous contribution to the concept of surface-confined foldamers revealed promising prospects

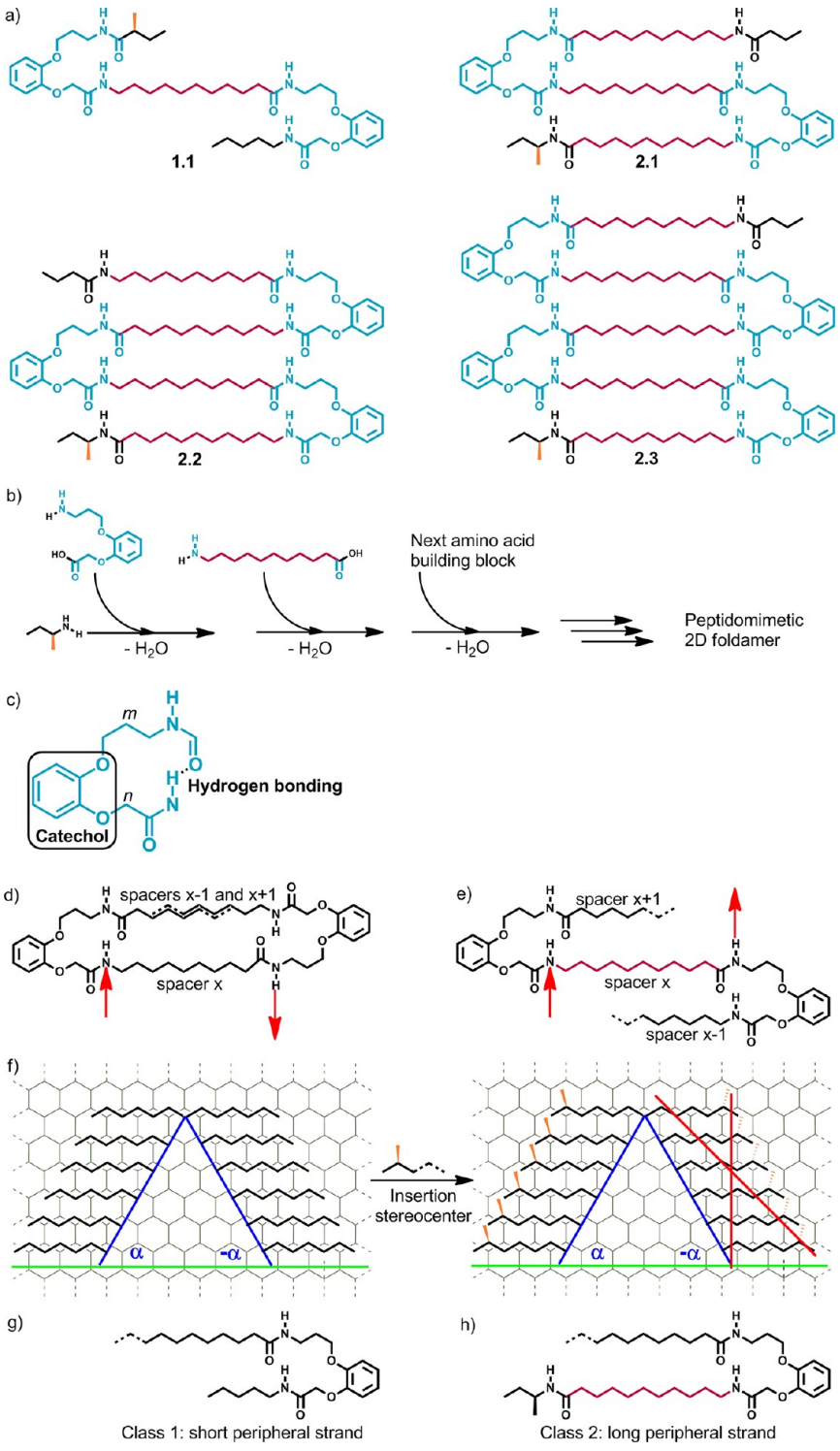

Figure 1. Molecular structures, stepwise synthesis, and design of oligomeric 2D foldamers. (a) Molecular structures of the extended foldamers with short peripheral strands, 1.1; two turn elements, 2.1; three turn elements, 2.2; and four turn elements, 2.3. (b) Schematic of a stepwise synthesis of peptidomimetic 2D foldamers. (c) Turn element for 2D foldamers with catechol as scaffold (inset) and hydrogen bonding between amides (dashed bond). (d, e) Lamellar spacer for 2D foldamers with even (d) and odd (e) numbers of methylene units. (f) Tentative model of mirror-image lamellar domains on the surface of graphite. Implementation of a stereocenter in the alkyl structure does not allow one of the two domains. (g, h) Foldamers of class 1 (g) and class 2 (h).

in employing the self-assembly of linear oligoalkyl amides as folding-on-surface building blocks for the precise 2D positioning of functional elements.[19,20] Oligoalkyl amides were chosen as basic structural motifs for this research since they are readily accessible *via* well-established methodologies used for peptide synthesis. Secondly,

they offer several inter- and intramolecular interaction sites, especially *via* hydrogen bonding, which could direct and stabilize their self-assembly. The amino acidic nature of the building blocks allows the application of the stepwise synthesis of peptides toward these oligomeric foldamers (Figure 1b), which can be considered as peptidomimetics (see Supporting Information for synthesis and technical procedures).

A basic part governing the conformation of a 2D foldamer is the turn element (Figure 1c), which enforces a 180° turn where the oligomeric sequence folds upon itself. In our earlier work, we designed, synthesized, and successfully evaluated the folding capability of a 2D turn mimic residue based on an amino acid bearing an *ortho*-catechol moiety with a 3-propylamine and a ω'-alkylcarboxylic acid.[20] The *ortho* substitution on the catechol moiety, which acts as a scaffold, directs the alkyl spacers to be parallel to each other.[19] It is already established that the spacer length (defined as *n* and *m*) between the amide and the catechol unit is a critical factor governing whether a given oligoamide sequence undergoes 2D folding upon adsorption on HOPG.[20] A variation in the spacer length affects the stability of hydrogen-bonding interactions between parallel and adjacent amides and hence the folding behavior. An oligoamide based on the rule $n = 1$ and $m = 3$ served as a minimal foldamer and formed a stable, well-ordered network at the 1-phenyloctane/HOPG interface. In general, these studies indicated that the structural matching of the turn elements and the intramolecular noncovalent interactions have a strong bearing on the 2D folding behavior of oligoamides.[19,20]

Having developed the turn element conducive for 2D folding upon surface confinement, the next challenge is to apply the established design to an extended sequence which consists of more than one turn element. This objective merits an extremely careful design of the long alkyl spacer, which is the second main structural element (Figure 1e, purple) and represents the core component for the lamellar assembly (defined as "lamellar spacer"). Care needs to be taken for its design since an odd number of methylene units in this spacer *X* (presuming it takes the stable all-*trans* conformation on the surface) is likely to set the two lamellar H-bonding arrays antiparallel (see red arrows in Figure 1d), thus undesirably overlapping spacer $x-1$ to the subsequent spacer $x+1$. On the other hand, in view of well-known two-dimensional odd/even effects in lamellar assemblies[40,41] an even number of methylene units will force the H-bonding arrays parallel (Figure 1e), warranting a 2D oligomeric serpentine sequence.

A third aspect to increase the level of control on the 2D supramolecular assembly is the implementation of a stereocenter in the oligoalkyl amides. Alkyl compounds can form mirror-image lamellar domains (Figure 1f) in which the lamella axis (blue) can be oriented at a positive ($+\alpha$) or negative ($-\alpha$) angle with respect to one of the main symmetry axes of graphite (green). Introduction of a stereogenic center in the molecular structure does not allow the formation of one of the two domains,[42] thus increasing the level of control. Finally, class 2 (Figure 1h) differs from class 1 (Figure 1g) for the longer peripheral alkyl strands, ideally allowing for a stronger interaction with HOPG.

2D Folding and Assembly Behavior at the Liquid−Solid Interface. The structural turn element and secondary amide groups are integrated into the molecular structure to ensure that these oligomeric sequences undergo 2D folding upon adsorption at the liquid−solid interface. Moreover, each modular unit is further capable of intermolecular hydrogen bonding to form extended network of molecules. The alkyl chains of the foldamers are expected to stabilize the self-assembled network *via* favorable molecule−substrate interactions, which are mainly van der Waals in nature. Such "soft" epitaxial stabilization of alkylated molecules on the surface of HOPG has been widely confirmed.[43−45] Whether a balance of all these interactions indeed leads to intramolecular folding and extended network formation was investigated by using STM at the liquid−solid interface. In view of relatively lower solubilities of foldamers, saturated solutions were prepared in 1-octanol by gentle heating at 60 °C. A droplet of this solution at room temperature was then applied onto the basal (0001) plane of HOPG. The interfacial adsorption and self-assembly behavior of the foldamers were then examined by STM at the 1-octanol/HOPG interface.

Since the interpretation of STM images could become complicated with an increase in the length of foldamers, we first introduce our approach toward the analysis of the STM data. Figure 2 shows simplified models for the expected columnar arrangement of different oligoamides upon adsorption in a folded conformation. Such structures are envisioned based on our previous investigations[19,20] of similar (minimal) foldamers, which showed that the foldamers form columnar patterns with head-to-head arrangement of catechol units that typically show up as bright blobs in STM images. Thus, a line profile drawn through such bright spots will furnish us the number of catechol units adsorbed in a given column. A corresponding line profile through the alkyl chain region (approximately perpendicular to the alkyl chains) will then give us the number of alkyl chains adsorbed on the surface per catechol unit. Each schematic shows the expected number of alkyl chains adsorbed on the surface per catechol unit for a given foldamer. For different foldamers this number will vary as depicted in the schematics shown in Figure 2.

Upon adsorption at the 1-octanol/HOPG interface, **1.1** forms 2D columnar structures that are rather fragile assemblies and are easily disrupted by the scanning

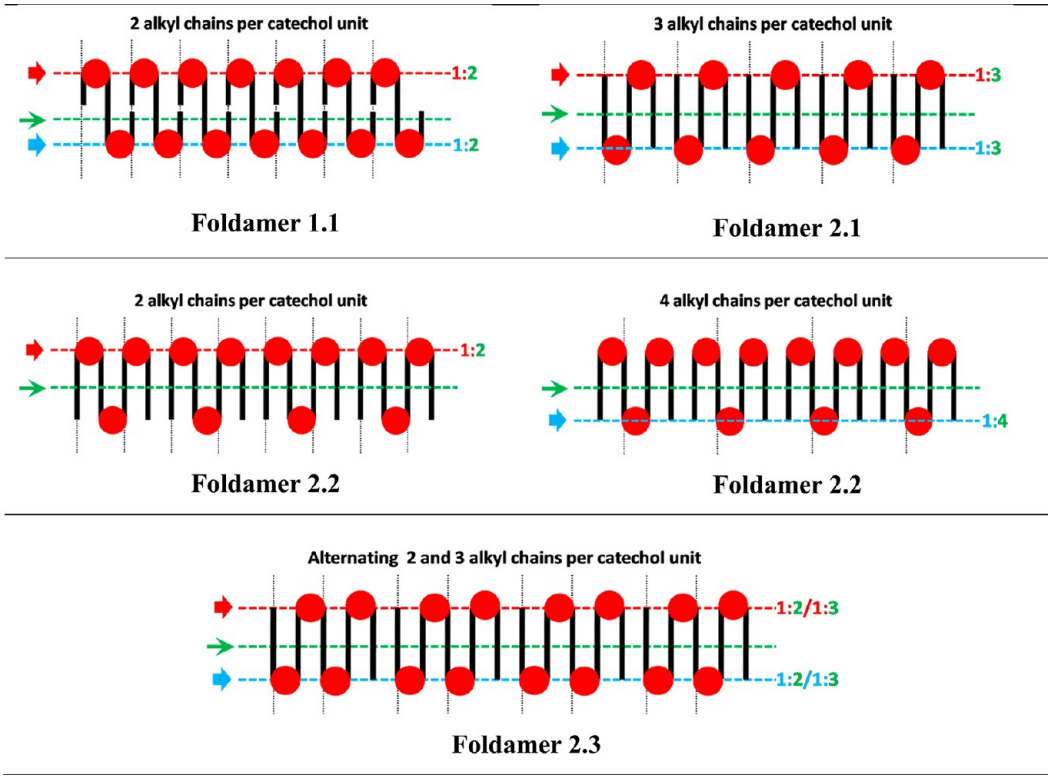

Figure 2. Schematics showing the number of alkyl chains adsorbed on the surface per catechol unit expected from a 2D folded arrangement of different foldamers. Red circles indicate catechol units, whereas the black solid lines show alkyl chains. The number can be obtained from the line profiles drawn through the catechol units (red and blue dashed lines) and then comparing it with the corresponding profile through the alkyl chain region (green dashed lines). Except for the case of 2.2, the folded structures are symmetric in the sense that they present an equal number of catechol units on either side of the column. Thus, for foldamers 1.1 and 2.1, the alkyl chain count per catechol will be 2 and 3, respectively, whereas for the foldamer 2.3 this number will vary alternately between adjacent catechol units. For 2.2 this number will be either 4 or 2 alkyl chains per catechol unit depending on which side of the column it is measured (2 if measured along the red dotted line and 4 if measured along the blue dotted line).

tip. Figure 3 shows STM images in which the molecules of **1.1**, which consists of two turn elements with short peripheral strands, are arranged in close packed columns. The periodicity of bright features appearing in the STM images is 2.18 ± 0.06 nm. The high-resolution STM (HR-STM) image in Figure 3b clearly shows the presence of bright blobs along the column axis and striped features in between these bright rows. The bright features correspond to the catechol groups of **1.1**, whereas the striped features arise from the alkyl chains. The alkyl chains make an angle of (61 ± 2.0°) with the column axis, and they are oriented along one of the main symmetry axes of HOPG. The line traces through the bright features and alkyl chain region along the column axis provide a profile as shown in Figure 3c. It can be easily noticed that there is a one to one correspondence between these features, indicating that there is only one alkyl chain adsorbed on the surface of HOPG per catechol unit. This observation does not conform to the expected folded conformation of **1.1** on the surface as proposed in Figure 2.

Considering the information obtained from line profile analysis and based on the periodicity of the columnar structures, a molecular model was built as shown in Figure 3d. The model depicts that the molecules of **1.1** are adsorbed on the surface in an unfolded conformation with their catechol units standing upright, perpendicular to the HOPG surface. Thus, no in-plane folding takes place. Even in such an unfolded conformation, molecules adsorbed in a given column can interact with each other *via* intermolecular hydrogen bonding interactions between their secondary amide groups and π-stacking interactions between the catechol moieties. The unit cell of **1.1** adsorbed at the 1-octanol/HOPG interface consists of 1 molecule/unit cell with $a = 4.30 \pm 0.06$ nm, $b = 0.52 \pm 0.04$ nm, and $\alpha = 89.8 \pm 1.5°$.

In contrast to **1.1**, foldamer **2.1**, bearing two turn elements with extended peripheral alkyl strands, forms a stable, close-packed structure on HOPG. Figure 4 shows representative large-scale and HR-STM images of foldamer **2.1** physisorbed at the 1-octanol/HOPG interface. The self-assembled monolayer of **2.1** emerges with columnar features with a clear distinction between well-defined regions of bright and dark contrast. Adjacent domains of columns make angles of ~120° with respect to each other (Figure 4a), indicating the influence of substrate registry on molecular adsorption.

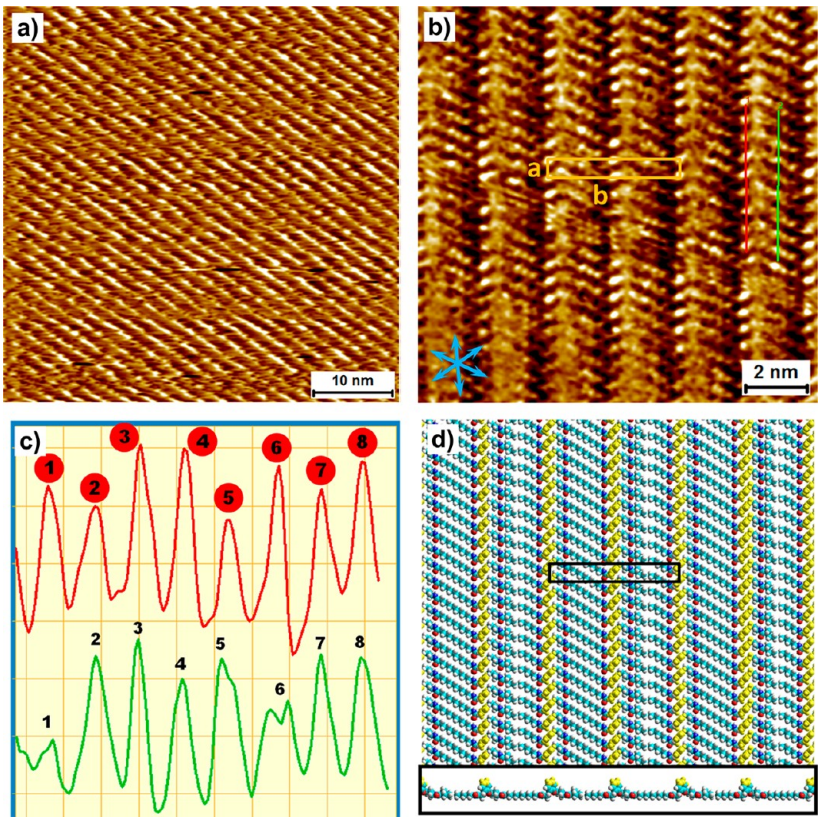

Figure 3. Large-scale (a) and HR-STM (b) images of 1.1 physisorbed at the 1-octanol/HOPG interface. The main symmetry axes of graphite are indicated in the lower left corner of (b). Imaging conditions: I_{set} = 140 pA, V_{bias} = −1.15 V. (c) Line profile along the red and green lines shown in the HR-STM image in (b). (d) Proposed molecular model. The catechol units stand upright and are shown in yellow color. Inset shows a side view of the molecular model.

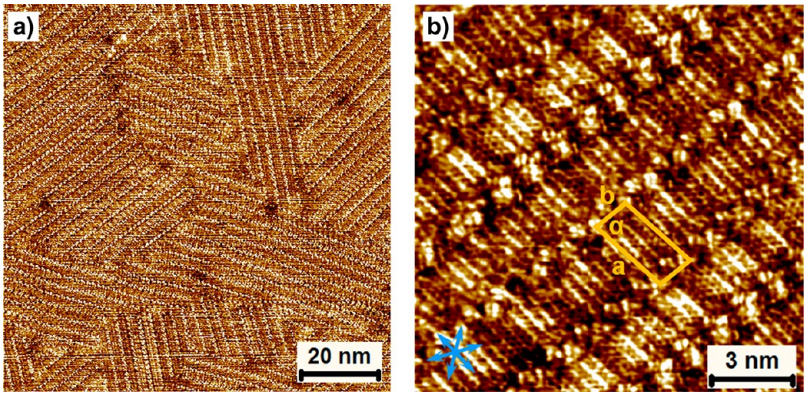

Figure 4. Large-scale (a) and high-resolution (b) STM images of 2.1 physisorbed at the 1-octanol/HOPG interface. The unit cell parameters are $a = 1.47 \pm 0.06$ nm, $b = 2.98 \pm 0.05$ nm, and $\alpha = 86.2 \pm 2.5°$. The main symmetry axes of graphite are indicated in the lower left corner of (b). Imaging conditions: I_{set} = 200 pA, V_{bias} = −400 mV.

A submolecularly resolved STM image of **2.1** shown in Figure 4b allows us to discern the microscopic aspects of these columnar structures. The bright blobs, which are arranged in a zigzag fashion, correspond to the catechol units. The striped features in between the rows of catechol units arise from the alkyl spacers of the foldamer. The STM contrast provides no direct information on the position and orientation of the secondary amide groups. The alkyl chains of the foldamer are particularly well-resolved in Figure 4b. They appear to be fully extended and closely packed and are always oriented along one of the main symmetry axes of the underlying graphite lattice. The distance between adjacent and parallel alkyl chains is 0.49 ± 0.05 nm. The width of the column is 2.85 ± 0.08 nm, which agrees closely with the folded columnar arrangement of molecules. The orientation of the alkyl chains with respect to the column axis is 89.3 ± 2.0°, and the columns in turn make an angle of +3.2 ± 1.2° with the normal to the symmetry axis of graphite (that is, the

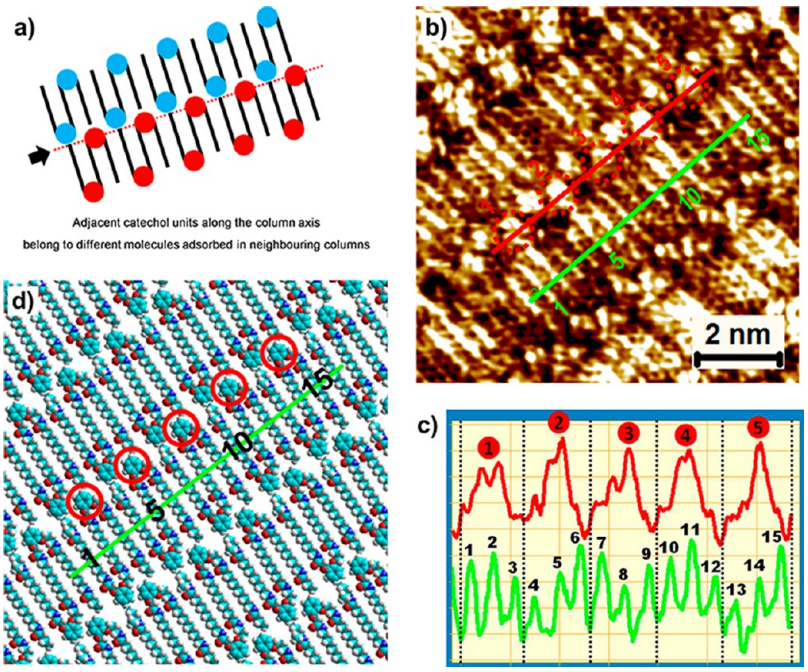

Figure 5. (a) Schematic showing the expected folded arrangement of 2.1. (b) HR-STM image of 2.1 and (c) corresponding line profile analysis in accordance with the scheme displayed in (a). (d) Proposed molecular model.

$\langle 1\bar{1}00 \rangle$ directions). A unit cell can be drawn with $a = 1.47 \pm 0.06$ nm, $b = 2.98 \pm 0.05$ nm, and $\alpha = 86.2 \pm 2.5°$.

In order to establish whether the molecules of **2.1** are adsorbed in a folded conformation on the surface, the following exercise was carried out. Figure 5a shows a schematic of the expected periodic columnar arrangement of **2.1** upon adsorption in a folded conformation. Molecules adsorbed in adjacent columns are depicted in different colors for the sake of clarity. Based on this schematic, it can be easily inferred that adjacent bright spots in the HR-STM image (Figure 4b) correspond to the catechol moieties belonging to different molecules of **2.1** adsorbed in neighboring columns. Thus, a line profile drawn through nonadjacent bright spots should correspond to the catechol moieties adsorbed in a given column. A corresponding line profile drawn through the alkyl chain region will then give us the number of alkyl chains adsorbed per catechol unit as described earlier. Thus, if the molecules of **2.1** adsorb in a folded conformation on the surface, then one expects three alkyl chains per catechol unit (Figure 2). The HR-STM image was analyzed in this fashion as shown in Figure 5b, c.

The line profile analysis (Figure 5c) clearly shows the presence of three alkyl chains per catechol unit, thus confirming the folded conformation of **2.1** on the surface. In addition, the periodic appearance of three alkyl chains per catechol also confirms the well-ordered assembly of this foldamer on the surface. Figure 5d shows a molecular model that reproduces the observed packing and symmetry and is based on the information obtained from the line profile analysis. This analysis is further supported by the fact that the distance between nonadjacent catechol units along the column axis is ~1.5 nm, which is consistent with the adsorption of three parallel alkyl chains with an interchain distance of ~0.5 nm (*vide supra*).

The line profile analysis shown in Figure 5 could be successfully applied to different STM images (Figure S1 in SI) and corroborates the fact that **2.1** adsorbs in a folded conformation to form an extended well-ordered network on the HOPG surface. A characteristic feature of this monolayer is that relatively strong inter- and intramolecular interactions exist only along the column axis, whereas the interactions between adjacent columns (perpendicular to the column axis) are based on rather weak van der Waals forces. As a consequence, the catechol moieties sometimes appear differently shifted with respect to each other. The monolayer shows intermittent defects in the form of missing catechol units, indicating their partial desorption and/or out-of-plane rotation. (Figure S3 in SI) Additional evidence for intramolecular folding is obtained by STM imaging of domain boundaries where a single row of catechol units is visualized at the domain edge instead of a double row of zigzag-arranged pairs (Figure S5 in SI), confirming the molecular arrangement as proposed in Figure 5d.

To confirm the constitution of foldamer **2.2** at the 1-octanol/HOPG interface, HR-STM images were carefully scrutinized. The molecular structure of **2.2** consists of three turn elements, and thus a folded structure with three in-plane turns is expected. Figure 6 shows an HR-STM image of **2.2** along with detailed line profile analysis. The image shows a compact arrangement of molecules. The catechol units as well as the alkyl chains

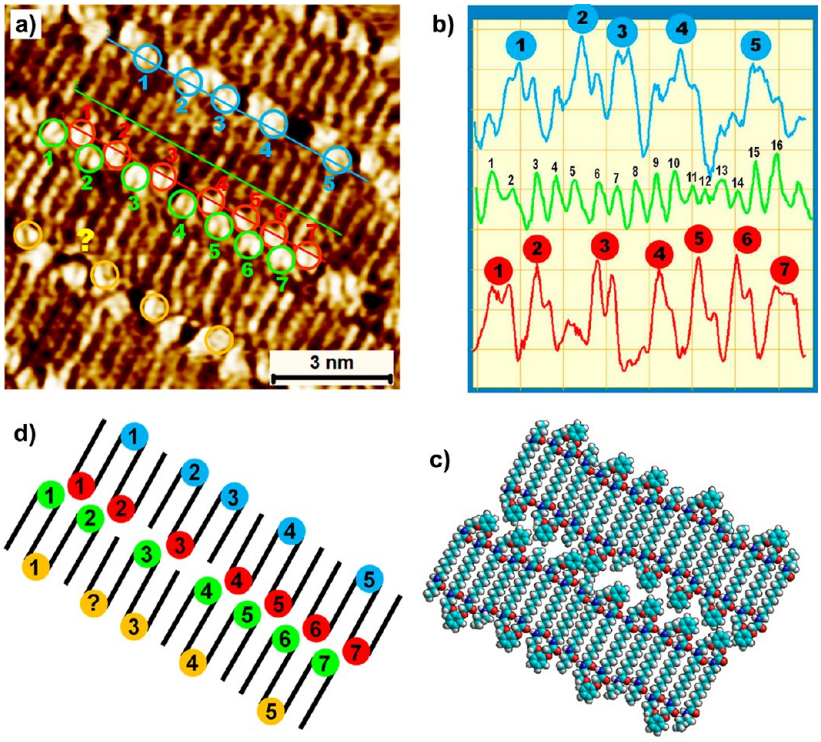

Figure 6. (a) HR-STM image of the monolayer formed by 2.2 at the 1-octanol/HOPG interface. The dotted circles highlight the catechol units, which are colored differently for the sake of clarity. The blue and red solid lines pass through the catechol units, whereas the green-colored line passes through the corresponding alkyl chain region. All the markers are color coded with the line profile shown in (b). (b) Line profile analysis of the molecules highlighted in (a). (c) Proposed molecular model based on the line profile analysis. (d) Simple schematic showing the molecular arrangement.

are well-resolved. The distance between alkyl chains is 0.50 ± 0.05 nm, and they lie parallel to one of the main symmetry axes of graphite. The width of the column is 2.90 ± 0.10 nm, which agrees well with the size of the folded columnar arrangement of molecules. A number of defects could be visualized along the column axis where the catechol units are adsorbed. In general, monolayers formed by **2.2** lack long-range order when compared to those of **2.1**. The density of catechol units along a given column axis as well as in different columns is not uniform. For example, the bright spots are compactly arranged along the red solid line in Figure 6a compared to those along the blue line. Some catechol units could not be accounted for in this analysis, and they could be partially desorbed from the surface, as highlighted by a question mark in Figure 6a and d. Moreover, the line profile analysis indicates that the number of alkyl chains per catechol units is far from what is expected (Figure 2) from an ordered 2D arrangement of **2.2**. Figure 6b shows the presence of two to three alkyl chains per catechol unit, and this arrangement is random.

On the basis of the information obtained from this analysis, a molecular model could be built as shown in Figure 6c. It is evident from the model that molecules of **2.2** often flip within a column, thus giving rise to defects and nonperiodic arrangement of the bright spots in the STM images. The line profile analysis coupled with the molecular model confirms the in-plane folding of **2.2**. An important message from the analysis presented above is that although the molecules of **2.2** adsorb in the folded conformation, they are plausibly not well-ordered. This behavior remains the same irrespective of the location of analyzed molecules whether they are adsorbed in the middle of the domain or along the domain boundaries as shown in Figure S6 in the Supporting Information. Thus, the number of defects and disorder increase on going from the monolayer formed by foldamer **2.1**, which has two in-plane turns, to those formed by **2.2**, with three turns.

It must be noted at this juncture that these foldamers have a stereogenic center with a pendant methyl group. The molecular models presented in Figure 6c consist of molecules adsorbed with their methyl groups pointing away from as well as toward the surface of graphite. It has been argued in the recent past that the most bulky group on a stereogenic center present on an alkyl chain tends to be directed away from the graphite surface.[40] This rather intuitive guideline, however, must be considered in the context of each system. In the present case, an alternative arrangement in which all the molecules of **2.2** adsorb with their methyl groups pointing toward the solution phase leads to an unfavorable orientation of intermolecular hydrogen bonding sites. Analysis of alternative

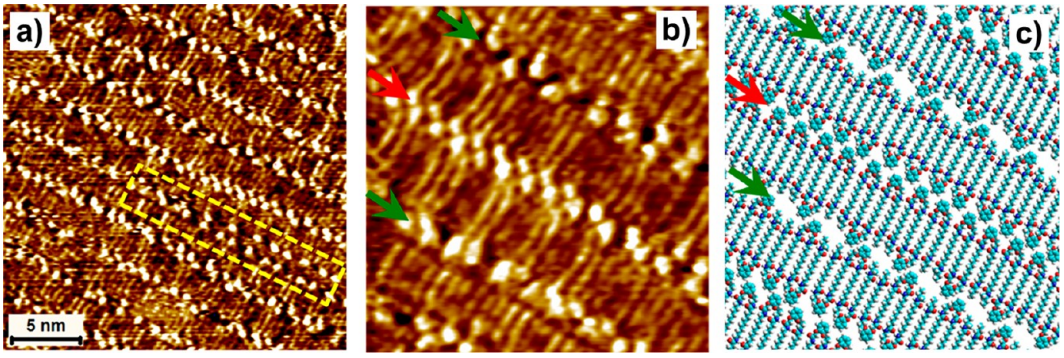

Figure 7. (a) STM image of 2.2 at the 1-octanol/HOPG interface showing large defects. The adjacent columns open up at such locations, giving rise to the "supramolecular zipper", as shown by the dotted rectangle. (b) The appearance of densely packed bright features (red arrow) is typically accompanied by loosely packed features on either side (green arrows) of the column. Such features arise due to local order in the columnar structure. (c) Tentative molecular model for the STM image depicted in (b).

models (Figures S6 and S7 in SI) of domain boundaries formed by **2.2** indicates that some of the molecules plausibly adsorb with their methyl substituents pointing toward the graphite surface, and in such an arrangement, the intermolecular hydrogen-bonding interactions are maximized. A similar exception has been noted recently in the case of supramolecular assemblies of chiral porphyrin derivatives where methyl groups present on the stereogenic center point toward the HOPG substrate.[46] Moreover, since the stereogenic center is located at the very end of the alkyl chain in the present case, it is also possible that the molecules adsorb with the methyl group on the surface, whereas the terminal ethyl group points up to the solution phase. This possibility, however, could not be verified from the analysis of calibrated STM images due to the very small difference in the lattice parameters expected from adsorption of molecules with either the methyl or the ethyl group on the surface.

Very often, STM images of **2.2** show adjacent columns that are shifted away from each other, as shown in Figure 7a. The monolayer in such regions appears to behave like a "supramolecular zipper", where adjacent columns move apart from each other, plausibly due to lack of strong intercolumnar interactions (*vide supra*). This shift also reveals the hierarchical nature of the self-assembly process of foldamers. The observation of such shifted columnar structures proves the prevalence of strong van der Waals and hydrogen-bonding interactions within a given column that are capable of stabilizing individual columns. Another characteristic feature of these monolayers is that the appearance of crowded bright features along one row in the monolayer is typically associated with loosely spaced bright features on either side of such a row, as shown in Figure 7b. This can be accounted for by considering relatively well-ordered patches of foldamer **2.2** that extend locally for a few nanometers before the disorder sets in. A molecular model depicting such an ordered array of **2.2** is shown in Figure 7c. A lack of long-range periodicity along either directions (along or perpendicular to the columns) precludes the assignment of a unit cell for monolayers of **2.2** formed at the 1-octanol/HOPG interface.

The disordered arrangement of **2.2** is an indication of the increasing complexity of supramolecular interactions involved in the adsorption process with increasing length of the oligomers. The decrease in the solubility of foldamers in 1-octanol with an increase in the molecular weight further complicates the matter. The longest foldamer of this study, foldamer **2.3**, is only sparingly soluble in 1-octanol, and hence chloroform was used as a cosolvent. The solutions of **2.3** were prepared in a mixture of 1-octanol and chloroform (1:1 v/v). The adsorption of **2.3** from such a mixture on the surface of HOPG leads to formation of columnar patches that extend a few tens of nanometers.

Figure 8 shows typical STM images of the monolayer formed by **2.3**. It reveals that the molecules are adsorbed in a columnar fashion akin to those of shorter foldamers. The catechol units are poorly resolved, and they typically appear as fuzzy features, indicating substantial in-plane dynamics on the time scale of STM measurement. Very often, patches of disordered structures could be observed as shown in the upper half of Figure 8b. Only a few aromatic units are resolved in the STM images presented in Figure 8, which are also indicative of a disordered arrangement. Repeated experiments on this system revealed that the monolayers remain dynamic and hence disordered for a long time and the relatively fast in-plane dynamics of molecules (especially of the catechol units) prevents the acquisition of high-resolution images. The high degree of in-plane dynamics in the monolayers of **2.3** is also evident from Figure 9, which shows sequential STM images that capture opening of a columnar structure as a function of time. Such opening could be spontaneous, or it could be scanning induced. The lack of well-resolved catechol units and/or a corresponding alkyl chain region further prevents the detailed line profile analysis that was employed to prove the in-plane folding of shorter foldamers. Nevertheless, the

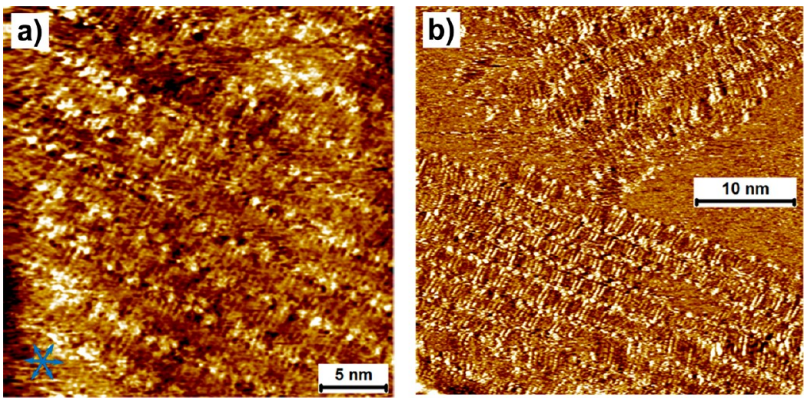

Figure 8. Typical STM images of foldamer 2.3 adsorbed at the 1-octanol/HOPG interface. The catechol groups could not be well-resolved, possibly in view of their fast in-plane dynamics on the time scale of STM measurements. The arrangement of molecules within individual columns appears to be random. A disordered arrangement at the level of domain can be seen in the upper part of (b).

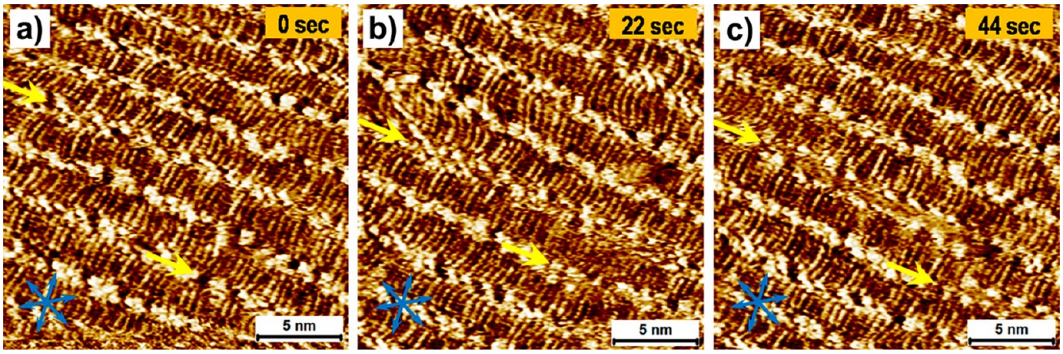

Figure 9. Sequence of STM images showing substantial surface dynamics present in the monolayers of 2.3 at the 1-octanol/HOPG interface. Yellow arrows indicate the lines along which the columns start shifting away from each other.

surface patterns formed by **2.3** appear structurally similar to those obtained with foldamer **2.2**, and thus there is a possibility that the molecules of **2.3** also adsorb in a folded conformation on the surface.

To induce order in the monolayers of **2.3**, HOPG was heated at 60 °C for a few minutes followed by rapid evaporation of 1-octanol at higher temperatures. The STM imaging was then carried out by adding a drop of neat 1-phenyloctane, which is a nonsolvent for the molecules of **2.3**. Such an experiment leads to the formation of highly ordered domains of molecules as depicted in Figure 10a. The HR-STM image presented in Figure 10b reveals a well-ordered arrangement of molecules. The bright spots that are indicative of the catechol moieties appear in groups of four, as expected from an ordered arrangement of foldamer **2.3**. The alkyl chains are aligned along one of the symmetry axes of graphite. They are oriented approximately perpendicular to the column axis, and the columns in turn make an angle of $+3.0 \pm 1.5°$ with the normal to one of the main symmetry axes of the graphite lattice.

The line profile (Figure 10c) indicates that the molecules indeed adsorb in a folded conformation. A peculiar periodic arrangement of alternating three and two alkyl chains per catechol units is evident in the line profile. It must be noted that such an arrangement is predicted in the schematics shown in Figure 2 for the well-ordered 2D packing of **2.3** on the surface. A molecular model that reproduces the observed packing and symmetry in the STM images is given in Figure 10d. The model clearly shows that each molecule of **2.3** adapts a conformation with four in-plane turns, and the intramolecular hydrogen-bonding interactions further facilitate the formation of an extended network.

As mentioned earlier, this investigation is a culmination of our previous studies wherein we validated the design of the peptidomimetic oligomers that could fold upon surface confinement. The foldamer design employed here is a rational extension of the minimal foldamer[20] reported by us earlier. Thus, a few experimental facts established during the earlier studies deserve a mention. Molecular modeling studies carried out on the minimal foldamer indicated that the folded state is favored compared to the unfolded state both on graphite and in a vacuum.[20] STM images confirmed that the minimal foldamer forms a stable self-assembled network in which the molecules are adsorbed in a folded conformation. Furthermore, systematic infrared (IR) spectroscopy measurements carried out in 1-phenyloctane proved that the minimal foldamer remains unfolded in solution and folding occurs only upon adsorption at

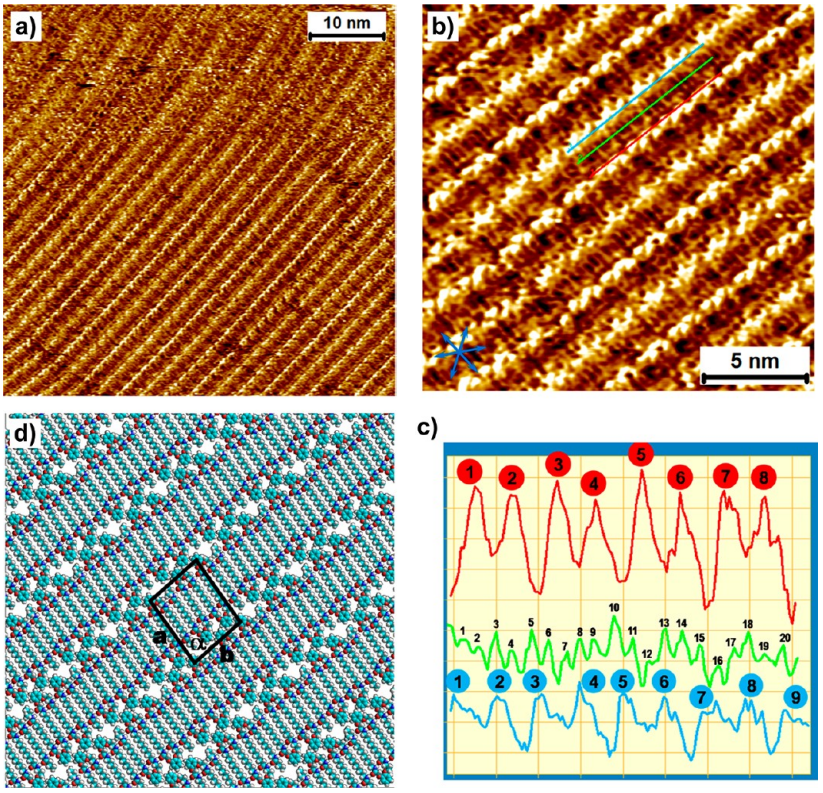

Figure 10. Large-scale (a) and HR-STM (b) images of 2.3 obtained after annealing the sample followed by rapid evaporation of 1-octanol at higher temperatures. A regular arrangement of foldamer 2.3 is evident from the STM images. (c) Line profile analysis along the colored lines in the STM images shown in (b). The line traces through different parts of the column corroborate the folded and periodic arrangement of 2.3 on the HOPG surface. (d) Tentative molecular model. Unit cell parameters are $a = 3.08 \pm 0.08$ nm, $b = 2.60 \pm 0.05$ nm, $c = 90.3 \pm 1.5°$ Imaging conditions: $I_{set} = 120$ pA, $V_{bias} = -825$ mV.

the liquid/solid interface. This was confirmed by following the −N−H stretching region in the IR spectra of foldamers in 1-phenyloctane and dichloromethane in a systematic concentration-dependent experiment. Since the intramolecular hydrogen bond formation between the secondary amide groups is necessary for folding, the −N−H stretching region provided a marker of whether or not the molecules form intramolecular hydrogen bonds leading to a folded conformation.

Unfortunately, similar experimental verification of the conformational state of the extended foldamers (i.e., intramolecular H-bonding formation) is not feasible in 1-octanol due to the overlap of the broad hydroxyl (−OH) band of the solvent with the −N−H stretching region of the foldamers. Nevertheless, FTIR measurements on dilute dichloromethane solutions of the shortest and the longest extended foldamers studied in this work, compounds **2.1** and **2.3**, displayed similar spectra to those previously observed for minimal foldamers bearing the same turn mimic moiety.[20] The IR spectra display only a sharp peak at 3407 cm^{-1} (see Section 3 in SI), representative of −N−H groups exclusively interacting with dichloromethane.[47,48] This confirms that the monomeric extended foldamers do not form intramolecular hydrogen bonds in dichloromethane. Because 1-octanol is more strongly competing for hydrogen bonds than dichloromethane, we conclude that extended foldamers in their monomeric state do not form intramolecular hydrogen bonds and remain unfolded in 1-octanol as well.

DISCUSSION

The STM results for the extended foldamers described above indicate that, except for **1.1**, all the other foldamers exhibit in-plane folding. Although **1.1** assembles into a monolayer, its molecules do not fold at the liquid−solid interface and adsorb in an extended conformation. Among those foldamers that do undergo in-plane folding, there are distinct differences in the self-assembling behavior. Foldamer **2.1** forms a well-ordered network at the liquid−solid interface, whereas **2.2** and **2.3** exhibit a characteristic disordered assembly. It is well-established that the thermodynamics of the folding process involves a complex interplay between two important factors: enthalpy and conformational entropy. The enthalpic gain of intramolecular interactions in the folded state must compensate for the loss of conformational entropy upon folding.[26] In the present case, the loss of conformational entropy upon folding is expected to increase with the length of the foldamers. Thus, the entropic cost of folding should follow the order **1.1** < **2.1** < **2.2** < **2.3**. Since the molecules adsorb on the surface to form an extended network, the present case also involves additional loss

of rotational, vibrational, and translational entropy. On the other hand the enthalpic interactions are expected to increase with increasing molecular weight of the foldamers. Thus, the enthalpic gain follows the order **1.1** < **2.1** < **2.2** < **2.3**.

Despite the expected lower entropic cost of folding for **1.1**, it does not undergo in-plane folding. This implies that the enthalpic interactions for the folded structure of **1.1** are plausibly not sufficient to compensate for the loss of conformational entropy upon folding. Nevertheless, in the case of the remaining foldamers, folded structures are observed. This indicates that the enthalpic gain is a major thermodynamic factor governing the adsorption, folding, and extended network formation. This gain in enthalpy has contributions from the enthalpy of adsorption of individual molecules (dominated by molecule−substrate van der Waals interactions) and inter- and intramolecular interactions which comprise hydrogen bonding and van der Waals interactions between adjacent alkyl chains. Besides this, the lower solubilities of longer foldamers in 1-octanol point toward unfavorable enthalpies of solvation for these foldamers. Considering the fact that the enthalpy of adsorption is expected to be higher for longer foldamers, the difference in the adsorption and solvation enthalpies is expected to be relatively large and thus play a major role in the adsorption process. Thus, the higher entropic cost of folding for longer foldamers is more or less compensated by the enthalpic gain in the adsorbed (folded) state.

An overview of the results on this family of foldamers combined with those on minimal foldamer indicates that an increase in the molecular weight leads to formation of disordered networks. When molecules adsorb in an ordered fashion on the surface, one anticipates a significant loss of positional and orientational entropy. Thus, the networks formed by **2.2** and **2.3** clearly preserve their positional and orientational entropy in their noncrystalline packing. The source of the differential behavior of the foldamers appears to be mainly kinetic in origin, as indicated by the annealing experiments carried out on the monolayers of **2.3**. However, it must be noted at this juncture that the noncovalent interactions involved in the self-assembly process at the liquid−solid interface are highly reversible and thus generally warrant optimum conditions to achieve equilibrium and hence favor the formation of thermodynamically stable structures. The liquid phase acts as a reservoir of dissolved species, which can diffuse toward the substrate, adsorb, diffuse laterally, and desorb. This spontaneous dynamics is arguably one of the main advantages of self-assembly at this interface. Of great importance is the fact that these dynamic processes favor the repair of defects and disorder in general. In light of these aspects, the prevalence of kinetically trapped disordered structures for monolayers of **2.2** and **2.3** is rather surprising. Nevertheless higher enthalpic interactions with increased molecular size reduce the rate of adsorption−desorption dynamics,[48] which in turn leads to kinetically trapped structures. In fact, such kinetically trapped metastable structures and their transformation to thermodynamically stable forms have been observed in the recent past by employing STM.[6,47]

One must consider, however, the increasing complexity involved in both the folding and self-assembly process of progressively longer foldamers. The process of adsorption−desorption dynamics[48] is probably slowed down with an increase in the length of the foldamers, and the lengthier molecules appear to remain in the local potential minimum as soon as they form hydrogen bonds with their partners. The reduced solubility of longer foldamers in 1-octanol is further expected to decrease the rate of desorption dynamics once the molecules are adsorbed on the surface. A parallel can be drawn here between the 2D self-assembly and the condensation of molecules during the bulk crystallization process. Just as there are certain solid materials that undergo crystallization very efficiently, there are those that do not relax to their global thermodynamic minimum but form glasses instead. Such glassy materials are formed when the barrier for interconversion dominates the kinetics of relaxation.

In the present case, foldamers **2.2** and **2.3** efficiently find their folded state upon surface confinement; however the intermolecular hydrogen-bonding interactions between adjacent molecules tend to trap the kinetically formed structures in some kind of local potential minimum, thus preventing the formation of well-ordered domains of molecules and leading to the formation of a 2D molecular glass.[49,50] This observation indicates that though the increased enthalpic interactions are important for the stability of the supramolecular networks, they tend to immobilize the molecules at a faster rate, thus sacrificing the ability to heal the defects, which is a key step in the formation of well-ordered molecular networks. Nevertheless, as shown for the case of **2.3**, which is the longest foldamer investigated in this study, it is easily possible to construct ordered assemblies of foldamers by simple annealing.

Considering the initial goal of this study the results obtained are extremely promising. For compounds **2.1**, **2.2**, and **2.3** the folded state is always observed. This indicates that the design strategy works successfully at the level of folding of single molecules. However an important lesson from this investigation is that the design cannot be only limited to the level of single molecules, but 2D packing within a column and intercolumn interactions should also be considered explicitly. This is because the final state for the foldamers is not a folded or unfolded conformation but an extended network of the folded or unfolded conformation. To the best of our knowledge, this is the first study

that reports the 2D folding behavior of conformationally flexible foldamers with as many as four in-plane turns. Different functional groups can be appended on the ends of these foldamers, thus paving a way to functionalized surfaces with periodically positioned functional sites.

CONCLUSIONS

Surface-confined supramolecular networks of organic building blocks have been efficiently used in the recent past for the fabrication of patterned surfaces with periodicities at the lower end of the nanoscale. However, it remains a challenge to design modular systems that combine flexibility in the implementation of chemical functionalities, size, and symmetry. In order to overcome this challenge, we have successfully designed and synthesized a new class of oligoamide sequences that undergo in-plane folding when adsorbed at the organic liquid−solid interface. The interfacial adsorption of these oligomeric sequences was investigated by employing STM, which furnished submolecular resolution of both periodic and nonperiodic patterns. STM studies reveal that extended foldamers with long alkyl chains exhibit in-plane folding and extended network formation upon adsorption. This study shows that it is possible to control the spatial conformation of oligomeric molecules *via* noncovalent interactions such as hydrogen bonding and van der Waals interactions. These interactions could in turn be controlled by implementing specific functional groups *via* covalent synthesis. An overview of the STM results indicates that as the length of the foldamers increases, the self-assembly process becomes more and more kinetically driven, which leads to the formation of disordered networks that preserve the folded arrangement of molecules. A transition from disordered to well-ordered networks could be induced by simple annealing of the monolayer. The high spatial control over positioning of functional groups coupled with the modular nature of the building blocks provides a simple, efficient, and versatile route to surface patterning with nanometer-scale precision.

METHODS

STM Measurements. All STM experiments were performed at room temperature (20−23 °C) using a PicoLE (Agilent) machine operating in constant-current mode with the tip immersed in the supernatant liquid. STM tips were prepared by mechanical cutting from Pt/Ir wire (80%/20%, diameter 0.2 mm). Foldamers were dissolved in 1-octanol (Sigma-Aldrich 99%) by gentle heating at 60 °C. Compound **2.3** was dissolved in a mixture of chloroform (Aldrich 99%) and 1-octanol (1:1 v/v). Prior to imaging, a drop of the foldamer solution was applied onto a freshly cleaved surface of highly oriented pyrolytic graphite (grade ZYB, Advanced Ceramics Inc., Cleveland, OH, USA). The experiments were repeated in several sessions using different tips to check for reproducibility and to avoid experimental artifacts, if any. For analysis purposes, recording of a monolayer image was followed by imaging the graphite substrate underneath it under the same experimental conditions, except for lowering the bias. The images were corrected for drift *via* Scanning Probe Image Processor (SPIP) software (Image Metrology ApS), using the recorded graphite images for calibration purposes, allowing a more accurate unit cell determination. The images are low-pass filtered. The imaging parameters are indicated in the figure caption: tunneling current (I_{set}) and sample bias (V_{bias}).

Synthesis of Foldamers. All solvents were dried according to standard procedures. Starting materials were purchased from Aldrich or Acros. Solvent removal (bulk amount), unless differently specified in the procedure, was worked out at 45 °C, applying different vacuum with regard to the solvent. ^{1}H NMR and ^{13}C NMR spectra were recorded at 25 °C in $CDCl_3$ on a Varian Inova-300 (at 300 MHz for ^{1}H NMR and 75.42 MHz for ^{13}C NMR) and on a Bruker Advance-400 (at 400 MHz for ^{1}H NMR and 100.57 MHz for ^{13}C NMR). Chemical shifts were given relative to $CDCl_3$ (7.27 for ^{1}H NMR and 77.2 for ^{13}C NMR). The splitting patterns in the ^{1}H NMR spectra are designated as follows: s (singlet), d (doublet), t (triplet), m (multiplet), br (broad). MS (EI ionization) were performed on a Shimadzu GCMS-QP2010S system in EI+ ionization mode. MS (ESI+ ionization) were performed on a Shimadzu LCMS-2010A. Melting points were measured on an Electrothermal IA9300 apparatus. IR spectra were recorded on a Perkin-Elmer Spectrum One FT-IR spectrometer. Duplo (double) elemental analysis (C, H, and N) was determined using a Euro Vector 3400 CHN-S analyzer. The oxygen content was determined by difference. The data reported in the Supporting Information are the average of the double measurement. The synthesis and characterization of foldamers are described in detail in the Supporting Information.

Conflict of Interest: The authors declare no competing financial interest.

Acknowledgment. This work is supported by the Fund of Scientific Research-Flanders (FWO), K.U. Leuven (GOA 2006/2), Belgian Federal Science Policy Office (IAP 7-FS2), and an NWO VICI grant, The Netherlands. C.G. is thankful for an ERA Chemistry/NWO grant. The authors want to thank Dr. Jealemy Galindo Millan for the help with the graphical abstract.

Supporting Information Available: 1. Additional STM images and molecular models. 2. Materials and synthetic methods. This material is available free of charge *via* the Internet at http://pubs.acs.org

REFERENCES AND NOTES

1. Lewis, P. A.; Donhauser, Z. J.; Mantooth, B. A.; Smith, R. K.; Bumm, L. A.; Kelly, K. F.; Weiss, P. S. Control and Placement of Molecules *via* Self-Assembly. *Nanotechnology* **2001**, *12*, 231–237.
2. Hoeppener, S.; Chi, L. F.; Fuchs, H. Formation of Au-55 Strands on a Molecular Template at the Solid-Liquid Interface. *Nano Lett.* **2002**, *2*, 459–463.
3. Mao, G. Z.; Dong, W. F.; Kurth, D. G.; Mohwald, H. Synthesis of Copper Sulfide Nanorod Arrays on Molecular Templates. *Nano Lett.* **2004**, *4*, 249–252.
4. Elemans, J. A. A. W.; Lei, S. B.; De Feyter, S. Molecular and Supramolecular Networks on Surfaces: From Two-Dimensional Crystal Engineering to Reactivity. *Angew. Chem., Int. Ed.* **2009**, *48*, 7298–7332.
5. Ahn, S.; Matzger, A. J. Six Different Assemblies from One Building Block: Two-Dimensional Crystallization of an Amide Amphiphile. *J. Am. Chem. Soc.* **2010**, *132*, 11364–11371.
6. Ahn, S.; Matzger, A. J. Additive Perturbed Molecular Assembly in Two-Dimensional Crystals: Differentiating Kinetic and Thermodynamic Pathways. *J. Am. Chem. Soc.* **2012**, *134*, 3208–3214.

7. Wan, L. J. Fabricating and Controlling Molecular Self-Organization at Solid Surfaces: Studies by Scanning Tunneling Microscopy. *Acc. Chem. Res.* **2006**, *39*, 334–342.
8. Palma, C. A.; Cecchini, M.; Samori, P. Predicting Self-Assembly: From Empirism to Determinism. *Chem. Soc. Rev.* **2012**, *41*, 3713–3730.
9. Shen, Y. T.; Deng, K.; Zhang, X. M.; Feng, W.; Zeng, Q. D.; Wang, C.; Gong, J. R. Switchable Ternary Nanoporous Supramolecular Network on Photo-Regulation. *Nano Lett.* **2011**, *11*, 3245–3250.
10. Li, S. S.; Northrop, B. H.; Yuan, Q. H.; Wan, L. J.; Stang, P. J. Surface Confined Metallosupramolecular Architectures: Formation and Scanning Tunneling Microscopy Characterization. *Acc. Chem. Res.* **2009**, *42*, 249–259.
11. den Boer, D.; Habets, T.; Coenen, M. J. J.; van der Maas, M.; Peters, T. P. J.; Crossley, M. J.; Khoury, T.; Rowan, A. E.; Nolte, R. J. M.; Speller, S.; *et al*. Controlled Templating of Porphyrins by a Molecular Command Layer. *Langmuir* **2011**, *27*, 2644–2651.
12. Li, M.; Deng, K.; Lei, S. B.; Yang, Y. L.; Wang, T. S.; Shen, Y. T.; Wang, C. R.; Zeng, Q. D.; Wang, C. Site-Selective Fabrication of Two-Dimensional Fullerene Arrays by Using a Supramolecular Template at the Liquid-Solid Interface. *Angew. Chem., Int. Ed.* **2008**, *47*, 6717–6721.
13. Cavallini, M.; Albonetti, C.; Biscarini, F. Nanopatterning Soluble Multifunctional Materials by Unconventional Wet Lithography. *Adv. Mater.* **2009**, *21*, 1043–1053.
14. Madueno, R.; Räisänen, M. T.; Silien, C.; Buck, M. Functionalizing Hydrogen-Bonded Surface Networks with Self-Assembled Monolayers. *Nature* **2008**, *454*, 618–621.
15. Dri, C.; Peters, M. V.; Schwarz, J.; Hecht, S.; Grill, L. *Nat. Nanotechnol.* **2008**, *3*, 649–653.
16. Rothemund, P. W. K.; Folding, D. N. A. to Create Nanoscale Shapes and Patterns. *Nature* **2006**, *440*, 297–302.
17. Torring, T.; Voigt, N. V.; Nangreave, J.; Yan, H.; Gothelf, K. V. DNA Origami: A Quantum Leap for Self-Assembly of Complex Structures. *Chem. Soc. Rev.* **2011**, *40*, 5636–5646.
18. Sacca, B.; Niemeyer, C. M. DNA Origami: The Art of Folding DNA. *Angew. Chem., Int. Ed.* **2012**, *51*, 58–66.
19. Schuurmans, N.; Uji-i, H.; Mamdouh, W.; De Schryver, F. C.; Feringa, B. L.; van Esch, J.; De Feyter, S. Design and STM Investigation of Intramolecular Folding in Self-Assembled Monolayers on the Surface. *J. Am. Chem. Soc.* **2004**, *126*, 13884–13885.
20. Li, M.; Gobbo, C.; De Cat, I.; Eelkema, R.; Vanaverbeke, B.; Lazzaroni, R.; De Feyter, S.; van Escht, J. Molecular Patterning at a Liquid/Solid Interface: The Foldamer Approach. *Langmuir* **2011**, *27*, 13598–13605.
21. Khan, A.; Kaiser, C.; Hecht, S. Prototype of a Photoswitchable Foldamer. *Angew. Chem., Int. Ed.* **2006**, *45*, 1878–1881.
22. Meudtner, R. M.; Hecht, S. Helicity Inversion in Responsive Foldamers Induced by Achiral Halide Ion Guests. *Angew. Chem., Int. Ed.* **2008**, *47*, 4926–4930.
23. Yu, Z. L.; Hecht, S. Reversible and Quantitative Denaturation of Amphiphilic Oligo(azobenzene) Foldamers. *Angew. Chem., Int. Ed.* **2011**, *50*, 1640–1643.
24. Guichard, G.; Huc, I. Synthetic Foldamers. *Chem. Commun.* **2011**, *47*, 5933–5941.
25. Goodman, C. M.; Choi, S.; Shandler, S.; DeGrado, W. F. Foldamers as Versatile Frameworks for the Design and Evolution of Function. *Nat. Chem. Biol.* **2007**, *3*, 252–262.
26. Hill, D. J.; Mio, M. J.; Prince, R. B.; Hughes, T. S.; Moore, J. S. A Field Guide to Foldamers. *Chem. Rev.* **2001**, *101*, 3893–4011.
27. Gellman, S. H. Foldamers: A Manifesto. *Acc. Chem. Res.* **1998**, *31*, 173–180.
28. Lu, J. R.; Perumal, S.; Hopkinson, I.; Webster, J. R. P.; Penfold, J.; Hwang, W.; Zhang, S. G. Interfacial Nano-Structuring of Designed Peptides Regulated by Solution pH. *J. Am. Chem. Soc.* **2004**, *126*, 8940–8947.
29. Vankann, M.; Mollerfeld, J.; Ringsdorf, H.; Hocker, H. Amphiphilic Model Peptides: Circular Dichroism Measurements and Investigations by a Langmuir Balance. *J. Colloid Interface Sci.* **1996**, *178*, 241–250.
30. Zangi, R.; de Vocht, M. L.; Robillard, G. T.; Mark, A. E. Molecular Dynamics Study of the Folding of Hydrophobin SC3 at a Hydrophilic/Hydrophobic Interface. *Biophys. J.* **2002**, *83*, 112–124.
31. Fishwick, C. W. G.; Beevers, A. J.; Carrick, L. M.; Whitehouse, C. D.; Aggeli, A.; Boden, N. Structures of Helical Beta-Tapes and Twisted Ribbons: The Role of Side-Chain Interactions on Twist and Bend Behavior. *Nano Lett.* **2003**, *3*, 1475–1479.
32. Whitehouse, C.; Fang, J. Y.; Aggeli, A.; Bell, M.; Brydson, R.; Fishwick, C. W. G.; Henderson, J. R.; Knobler, C. M.; Owens, R. W.; Thomson, N. H.; *et al*. Adsorption and Self-Assembly of Peptides on Mica Substrates. *Angew. Chem., Int. Ed.* **2005**, *44*, 1965–1968.
33. Mao, X. B.; Wang, Y. B.; Liu, L.; Niu, L.; Yang, Y. L.; Wang, C. Molecular-Level Evidence of the Surface-Induced Transformation of Peptide Structures Revealed by Scanning Tunneling Microscopy. *Langmuir* **2009**, *25*, 8849–8853.
34. Ma, X. J.; Liu, L.; Mao, X. B.; Niu, L.; Deng, K.; Wu, W. H.; Li, Y. M.; Yang, Y. L.; Wang, C. Amyloid Beta (1−42) Folding Multiplicity and Single-Molecule Binding Behavior Studied with STM. *J. Mol. Biol.* **2009**, *388*, 894–901.
35. Liu, L.; Zhang, L.; Mao, X. B.; Niu, L.; Yang, Y. L.; Wang, C. Chaperon-Mediated Single Molecular Approach Toward Modulating a Beta Peptide Aggregation. *Nano Lett.* **2009**, *9*, 4066–4072.
36. Deng, Z. T.; Thontasen, N.; Malinowski, N.; Rinke, G.; Harnau, L.; Rauschenbach, S.; Kern, K. A Close Look at Proteins: Submolecular Resolution of Two- and Three-Dimensionally Folded Cytochrome c at Surfaces. *Nano Lett.* **2012**, *12*, 2452–2458.
37. Shen, Y. T.; Zhu, N. B.; Zhang, X. M.; Deng, K.; Feng, W.; Yan, Q. F.; Lei, S. B.; Zhao, D. H.; Zeng, Q. D.; Wang, C. A Foldamer at the Liquid/Graphite Interface: The Effect of Interfacial Interactions, Solvent, Concentration and Temperature. *Chem.—Eur. J.* **2011**, *17*, 7061–7068.
38. Jester, S. S.; Shabelina, N.; Le Blanc, S. M.; Hoger, S. Oligomers and Cyclooligomers of Rigid Phenylene-Ethynylene-Butadiynylenes: Synthesis and Self-Assembled Monolayers. *Angew. Chem., Int. Ed.* **2010**, *49*, 6101–6105.
39. Jester, S. S.; Idelson, A.; Schmitz, D.; Eberhagen, F.; Hoger, S. Shape-Persistent Linear, Kinked, and Cyclic Oligo-(phenylene-ethynylene-butadiynylene)s: Self-Assembled Monolayers. *Langmuir* **2011**, *27*, 8205–8215.
40. De Cat, I.; Gobbo, C.; Van Averbeke, B.; Lazzaroni, R.; De Feyter, S.; van Esch, J. Controlling the Position of Functional Groups at the Liquid/Solid Interface: Impact of Molecular Symmetry and Chirality. *J. Am. Chem. Soc.* **2011**, *133*, 20942–20950.
41. Tao, F.; Bernasek, S. L. Understanding Odd-Even Effects in Organic Self-Assembled Monolayers. *Chem. Rev.* **2007**, *107*, 1408–1453.
42. Elemans, J. A. A. W.; De Cat, I.; Xu, H.; De Feyter, S. Two-Dimensional Chirality at Liquid-Solid Interfaces. *Chem. Soc. Rev.* **2009**, *38*, 722–736.
43. Ilan, B.; Florio, G. M.; Hybertsen, M. S.; Berne, B. J.; Flynn, G. W. Scanning Tunneling Microscopy Images of Alkane Derivatives on Graphite: Role of Electronic Effects. *Nano Lett.* **2008**, *8*, 3160–3165.
44. Bleger, D.; Kreher, D.; Mathevet, F.; Attias, A. J.; Schull, G.; Huard, A.; Douillard, L.; Fiorini-Debuischert, C.; Charra, F. Surface Noncovalent Bonding for Rational Design of Hierarchical Molecular Self-Assemblies. *Angew. Chem., Int. Ed.* **2007**, *46*, 7404–7407.
45. Mali, K. S.; Lava, K.; Binnemans, K.; Feyter, S. Hydrogen Bonding *Versus* van der Waals Interactions: Competitive Influence of Noncovalent Interactions on 2D Self-Assembly at the Liquid-Solid Interface. *Chem.—Eur. J.* **2010**, *16*, 14447–14458.
46. Iavicoli, P.; Xu, H.; Feldborg, L. N.; Linares, M.; Paradinas, M.; Stafstrom, S.; Ocal, C.; Nieto-Ortega, B. L.; Casado, J.; Navarrete, J. T. L.; *et al*. Tuning the Supramolecular Chirality of One- and Two-Dimensional Aggregates with the Number of Stereogenic Centers in the Component Porphyrins. *J. Am. Chem. Soc.* **2010**, *132*, 9350–9362.

47. Kim, K.; Plass, K. E.; Matzger, A. J. Kinetic and Thermodynamic Forms of a Two-Dimensional Crystal. *Langmuir* **2003**, *19*, 7149–7152.
48. De Feyter, S.; Xu, H.; Mali, K. Dynamics in Self-Assembled Organic Monolayers at the Liquid/Solid Interface Revealed by Scanning Tunneling Microscopy. *Chimia* **2012**, *66*, 38–43.
49. Zhou, H.; Dang, H.; Yi, J. H.; Nanci, A.; Rochefort, A.; Wuest, J. D. Frustrated 2D Molecular Crystallization. *J. Am. Chem. Soc.* **2007**, *129*, 13774–13775.
50. Tahara, K.; Ghijsens, E.; Matsushita, M.; Szabelski, P.; De Feyter, S.; Tobe, Y. Formation of a Non-Crystalline Bimolecular Porous Network at a Liquid/Solid Interface. *Chem. Commun.* **2011**, *47*, 11459–11461.